# Test Results for a $Nb_3Sn$ Dipole Magnet

A.F. Lietzke, R. Benjegerdes, S. Caspi, D. Dell'Orco, W. Harnden, A.D. McInturff, M. Morrison, R. M. Scanlan, C.E. Taylor, and J.M. van Oort
Lawrence Berkeley National Laboratory, Berkeley, California, 94720

*Abstract*--A cosine theta type dipole magnet using $Nb_3Sn$ conductor have been designed, built and tested. D19H is a two-layer dipole magnet with a $Nb_3Sn$ inner layer and a NbTi outer layer. Coil-pairs are connected with two of the four $Nb_3Sn$ splices in a high field region, and compressed by a ring and collet system. It trained well at 4.4K , but poorly at 1.8K. Strain gages revealed that the coil-ends were not loaded well enough for high field operation (after cool-down), so another thermal cycle is planned. The low end-load is believed to be the cause of several mysteries observed during operation. Except for the outer-layer 1.8K training difficulty, the magnet's operation was encouraging.

## I. Introduction

A major goal of the Superconducting Magnet Program at LBNL is the advancement of magnet technology for accelerator magnets. As it is presently necessary to work with brittle materials for B > 10 T, $Nb_3Sn$ is currently being investigated as a prototypical brittle superconductor. Two different $Nb_3Sn$ 50 mm (bore), 1m long dipole designs are being evaluated.

A four-layer $Nb_3Sn$ design (D20), is under construction, in an attempt to explore the 12-14 Tesla range. Its details have been published previously (2,3). The principal goals of D20 are: (1) reach a significantly higher B-field, (2) validate the technology required for these field levels, (3) provide a facility to test insertion coils made with other high-field superconductors.

A second magnet (D19H) was built to provide a faster test-bed for the new $Nb_3Sn$ magnet technology. It utilized the two-layer "D19" design that had been previously developed at the Lawrence Berkeley National Laboratory to reach 10T using NbTi at 1.8 K. This design was modified to replace the inner layer conductor with a Nb3Sn cable. Its details are published elsewhere in these proceedings [1]. The primary goals of D19H were: (1) demonstrate that $Nb_3Sn$ magnet coils can be produced efficiently (once the tooling and magnet structure have been developed), (2) evaluate the feasibility of ring and collet precompression of $Nb_3Sn$ coils, (3) evaluate the ramp-rate sensitivity of $Nb_3Sn$ coils, and (4) validate new magnet assembly technologies before more complicated and expensive magnets are attempted.

The first training results for D19H are reported below.

Manuscript received 27 August 1996.

This work was supported by the Director, Office of Energy Research, Office of High Energy and Nuclear Physics, High Energy Physics Division, U. S. Department of Energy, under Contract No. DE-AC03-76SF00098.

## II. Experimental Details

### A. Instrumentation

Each $Nb_3Sn$ coil had 15 voltage-taps, positioned in a manner to monitor four anticipated trouble regions: the pole turn (highest B-field), each of the three wedges (highest discontinuity-related strain), the mid-plane turn (highest stress), and each splice (joint resistance). The outer coil had only full-coil taps. All voltage-tap signals were processed by analog-derivative amplifiers (1V output for 100V/s input). "Fast-Imbalance" signals were produced by nulling a coil section against its closest neighbor. These signals assisted the determination of quench onset.

Each $Nb_3Sn$/NbTi splice was soldered under pressure with a eutectic flux for a distance of 100 mm. A twisted pair of wires was attached across each joint and monitored with an HP3458A voltmeter. A thermometer was also embedded within each splice-block to monitor any temperature rise.

Four strain gages (one/coil/layer) monitored the pole-turn pressures; and load-cells (six/end) monitored the strain on each of twelve end loading-pins.

### B. Test procedures

The temperature and resistance of each coil was monitored during cool-down and warm-up. The strain gages were also monitored to determine the timing and amount of cool-down loading losses. At 4.4K, the magnet was ramped to quench at a slow rate (5A/s), until we later discovered that 20A/s was equivalent for training. After establishing the existence of a thermally-limited plateau, the ramp-rate sensitivity was measured. After cool-down to 1.8K, the above sequence was repeated.

After warming the magnet, both end-loads were increased substantially, in preparation for another round of tests. Testing was aborted when the magnet failed a standard 700V hi-pot test and degraded to 210V (considered inadequate to safely extract energy from the magnet during quenching).

## III. Experimental Results

### A. Cool-down

Two different superconducting transitions were easily visible at the expected temperatures (Fig. 1). Both outer (NbTi) coil resistances decreased (RRR = 75) from their initial values (each 136 mohms). The inner coils differed by 4% at 300K (100 mohms, 96 mohms). This relative difference increased during cool-down to 0.33 mohms and 0.24 mohms, prior to transition. This yielded significantly different RRR-values (300 and 400, respectively).

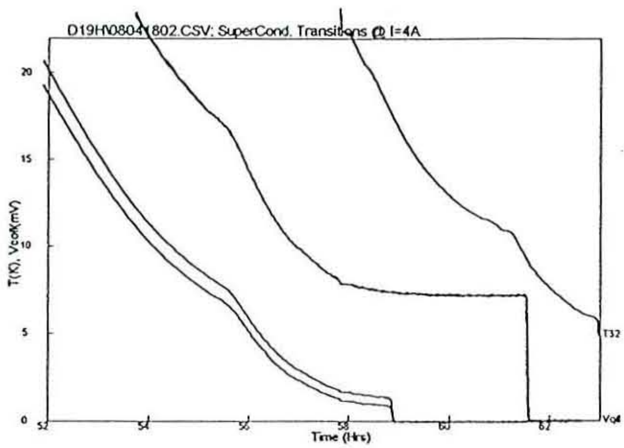


Fig. 1. The superconducting transitions of the inner (Nb3Sn, 18K) and outer (NbTi, 10K) coils were clearly differentiated during cool-down.

The strain-gages also changed during cool-down (Figs. 2, 3), showing an anticipated relaxation everywhere. The Lead-End nearly unloaded completely. During training, the outer pole pressures decreased from the initial 70-80 MPa preload (Fig. 4), while the inner gages and the ends increased (Fig. 5). After warm-up, all strain-gages indicated higher stresses than before cool-down. Two end-load increases were made before testing was aborted (failure to hold adequate voltage).

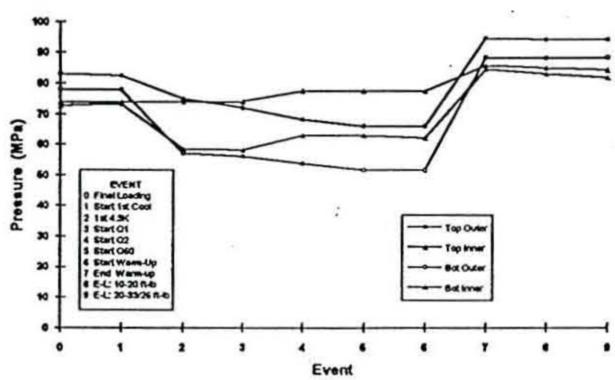


Fig. 2. Pole-Load history: Cool-down, training, warm-up, and re-loading.

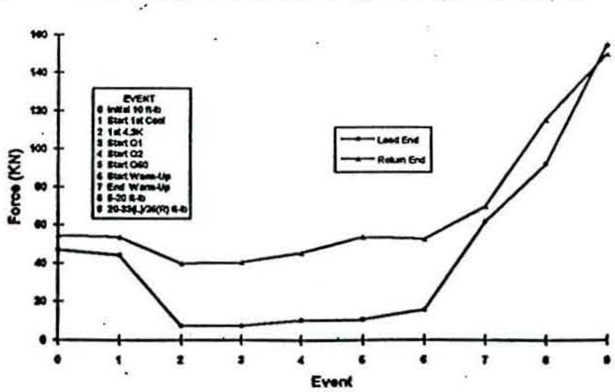


Fig. 3. End-Load history: Cool-down, training, warm-up, and two load increases.

*B. Training*

During ramping, the magnet transfer function was measured to be 1.13T/KA initially, reducing to 0.81 T/KA above 6T. The outer poles (Fig. 4) unloaded symmetrically with the square of the magnet current (excepting the first ramp). The inner poles were also symmetrical, but decreased nonlinearly above 8 Tesla. The end-loads increased nonlinearly (Fig. 5) at approximately 15% of the total Lorentz end-load.

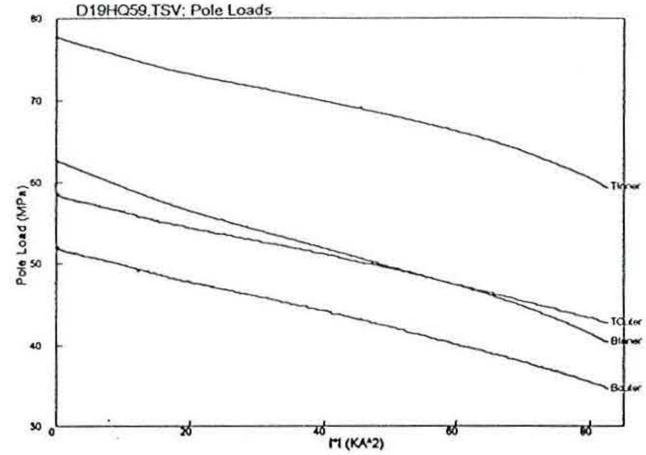


Fig. 4. The $I^2$ dependence of the pole strain-gauge signals was nearly linear for the outer layer, but not the inner layer (especially above 6 KA).

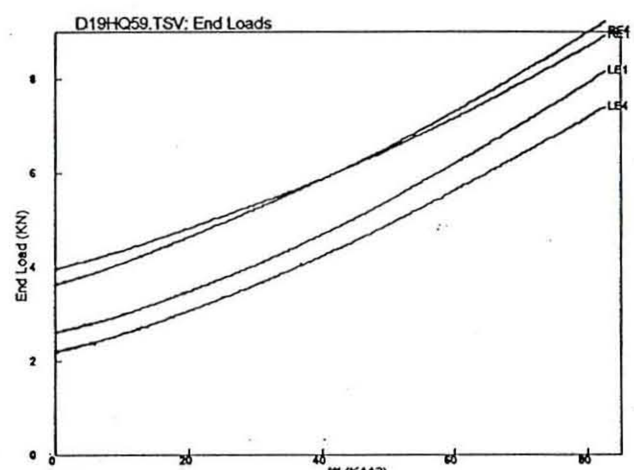


Fig. 5. The $I^2$ dependence of several end load-cell signals. They were non-linear for both ends.

The first 4.4K quench (Fig. 6) occurred at 7.4T (90% of plateau). Plateau was achieved after six outer layer quenches, one of which fell-back. The 1.9K training started with $Nb_3Sn$ (inner) coil quenching at a smaller fraction (80%) of the expected maximum (B>10T). The rate of improvement was significantly slower, and was dominated by outer (NbTi) coil quenching above ramp # 46. The frequency of "fall-backs" was also high. Training was aborted for 1.8K ramp-rate tests.

The quench onset is best identified with the "Fast-Imbalance" signals (Fig. 7, 8). Early 1.8K training quenches (Q26-46) were inner-layer quenches (Fig. 7 is typical) and seldom showed fast-motion signatures. They also showed a significantly (10x) smaller rate of resistance buildup than the outer-layer quenches. Figure 8 is typical for the limiting outer-layer quenches in the 1.8K training.

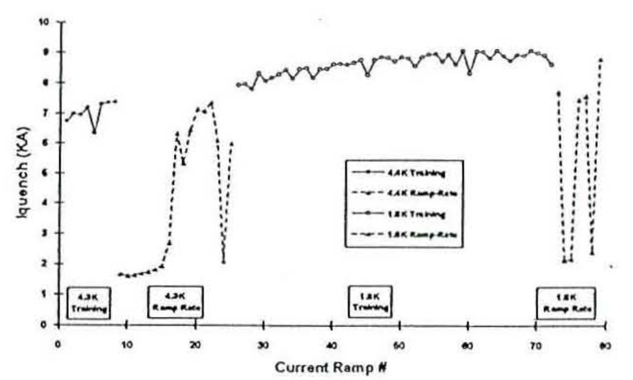


Fig. 6. Quench History: Training and ramp-rate studies at 4.4K and 1.8K. The 1.8K training was aborted to increase the end-load.

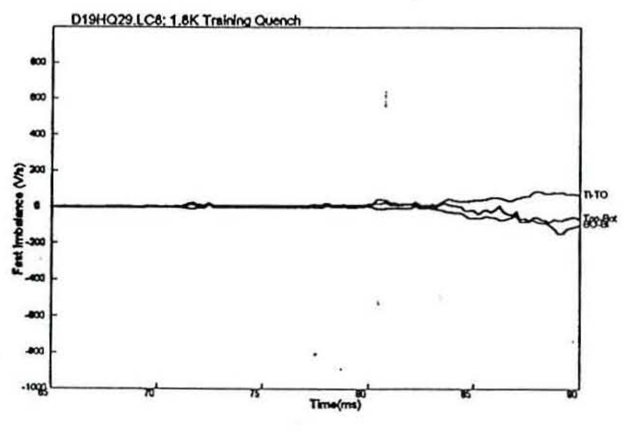


Fig. 7. Most of the first twenty 1.8K training quenches originated in the inner layer. They showed much smaller fast-motion imbalances and much slower quench propagation rates (7 m/s).

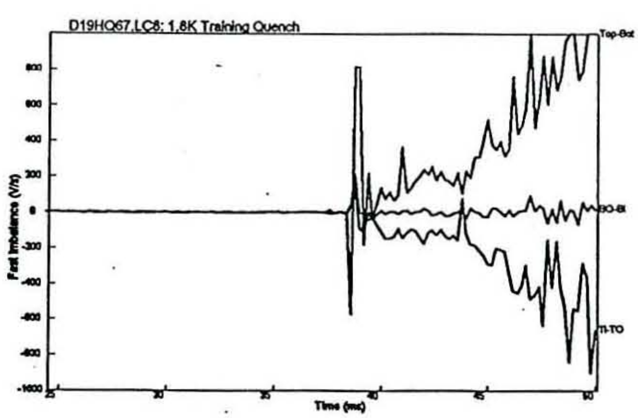


Fig. 8. The limiting 1.8K outer-layer training quenches typically showed large fast flux-imbalances, immediately before quench propagation.
TI-TO = Top(inner-outer) and BO-BI = Bot(outer-inner).

The number of Fast-Imbalance events increased rapidly with current during ramping (Fig. 9). At 4.4 K, most of them occurred shortly before the quench, the number reducing with training. At 1.8K, the rate of increase was more linear, starting at 5 KA. No decrease with training was observed above 7 KA.

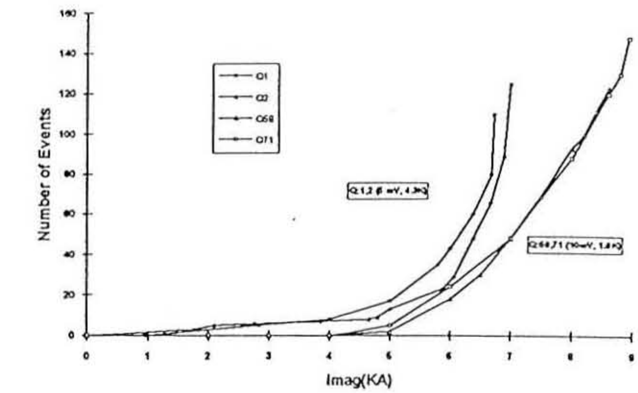


Fig. 9. Fast Imbalance Events: Total number vs. current (quenches Q1, 2 @ 4.3K had a threshold of 5 mV) (Q59, 71 @ 1.8K had a threshold of 10 mV).

The Fast-Imbalance history (Fig. 10) also illustrates the opposing trends of the two trainings. At 4.4K, the total number generally decreased, even though the current increased, while at 1.9K the total number increased with the current (and fell back when the current fell-back).

The splice resistances were independent of current, within the accuracy of the measurements. The pole splices (high field) showed a resistance (1 nano-ohm) that was three times the mid-plane average. The thermometers embedded in the copper splice blocks showed very small temperature rises (0-15 mK) during a 9 KA ramp (Fig. 11). One mid-plane splice showed only ramp-rate dependence, while one pole and the other mid-plane showed none. The pole-splice showed an ominous rate-of-rise around 8.5 KA. The other pole-splice was monitored with a germanium resistor, therefore giving unreliable readings in the magnetic field.

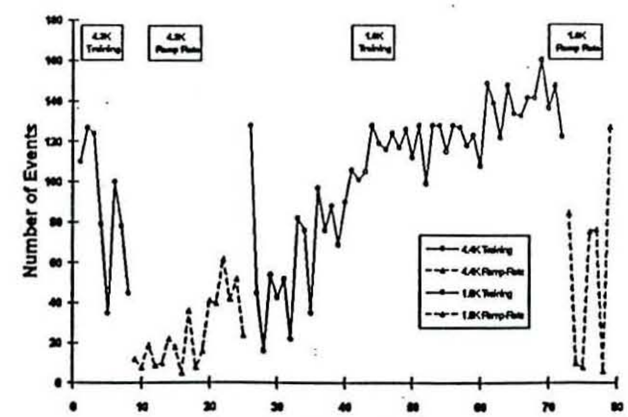


Fig. 10. Fast Imbalance History: Total number vs. Ramp #. The number generally decreased with training at 4.4K, but increased with current at 1.8K.

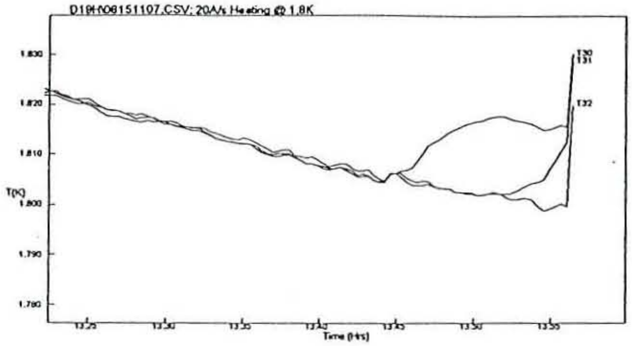


Fig. 11. The temperature history of three of the four $Nb_3Sn$/NbTi splices: One pole-splice showed a small ramp-rate sensitivity. One mid-plane splice showed a dramatically increasing current dependence starting 20% before quench. The other mid-plane splice only showed the quench.

The 4.4K ramp-rate sensitivity (Fig. 12) was weaker than anticipated from other reports[4], with an anomalous peak at 180 A/s, and a rapid fall-off at 200A/s to a plateau that was flat out to at least 1200 A/s. The 1.8K data also showed an even larger decline at a slightly higher ramp-rate (250 A/s), and a nearly identical plateau.

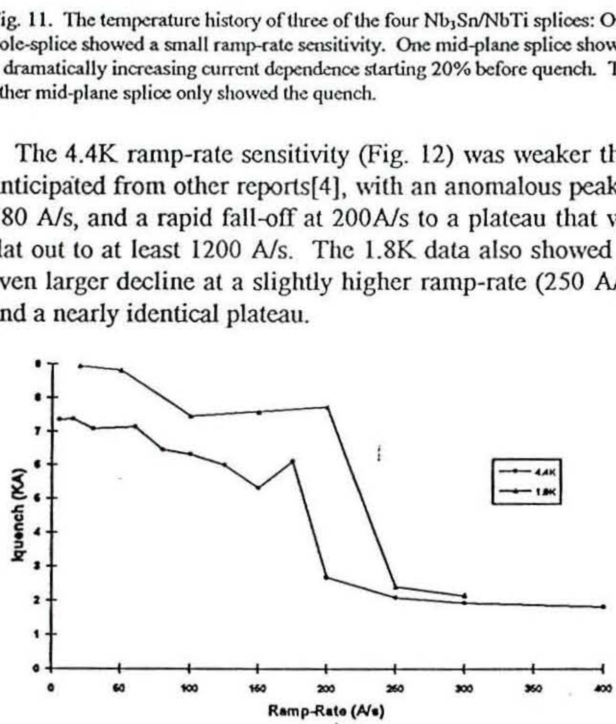


Fig. 12. Ramp-rate sensitivities at 1.8K and 4.4K: The 1.8K data below 200 A/s should be considered as lower-bounds only, as the associated quenches exhibited simultaneous outer-layer, fast imbalances at quench onset (implying outer-layer , motion-triggered quenching). The faster "plateau" quenches originated in a multi-turn section of the inner coil.

The voltage break-down discovered after warm-up was localized near the inner-to-outer-layer high-field splice in the bottom of the magnet. Testing was indefinitely terminated until this condition could be rectified.

## IV. Discussion

The slow 1.9K inner-coil training was dominated by the mid-plane turns. Several simultaneous upper and lower inner-coil quench-origins suggests the possibility of some mid-plane movement.

The fast-motion-dominated outer-coil training-limit and the persistently high number of outer layer fast-imbalances is strong evidence for inadequately loaded outer layer coils. This is believed to have been aggravated by the failure to stretch the outer layer during collaring (as was done for D19A), and the low total end-load applied simultaneously to two coils of markedly different stiffness[1]. The un-potted outer coil is apparently so loose as to even preclude fast-motion training (a prerequisite for increasing the quench-current).

The radial loading from the outside shell is believed to provide enough friction that only a fraction of the Lorentz load is delivered to the end-structure. The non-linear end-gage responses suggests that some of this friction is increasingly overcome as the Lorentz load increases.

The low cold lead-end-load resulted from the conservatively low initial end-load, coupled with the larger relative cool-down loss. As the epoxy-filled lead-end has twice as many parts and gaps, the larger relative plastic content in the lead-end is expected to produce a larger relative cool-down loss.

The slow $Nb_3Sn$ quench propagation speed is believed to indicate the existence of a large relative margin.

## V. Conclusion

A Nb3Sn/NbTi hybrid magnet was tested to validate several portions of our growing body of $Nb_3Sn$ coil technology. The magnet exhibited a pleasingly low ramp-rate sensitivity and low splice resistances, thereby validating our coil and splice technologies on these issues. The low $Nb_3Sn$ quench velocities validated our expectation of a high average margin for the inner conductor; but at 1.8K NbTi-coil training-ceiling limited our ability to extend observations to the 10.2 Tesla outer-coil limit. An uncharacteristically large number of outer-layer fast-motion events were recorded, leading us to suspect the unusually low end-loading. This could be tested by substantially improving the packing and loading of the outer coil. However, the cost/benefit ratio does not look favorable at present.

## Acknowledgments


The successful construction and testing of this magnet would not have been possible without the collective skills, expertise, and attention to detail contributed by the following persons: P. Bish (cryo-testing), R. Curtis (cryo-testing), S. Darden (coil reaction), R. Hannaford (coil winding, coil reaction & magnet assembly), H. Higley (cabling & magnet assembly), R. Oort (coil winding), J. Remenarich (coil-potting), and J. Smithwick (diagnostic assembly).


## References


[1] S. Caspi, et al., "Design and Construction of a Hybrid-$Nb_3Sn$", NbTi-Dipole Magnet, paper LKA-2 in these proceedings.

[2] R. M. Scanlan et al., "Fabrication and Component Testing Results for a $Nb_3Sn$ Dipole Magnet", *IEEE Trans. on Applied Superconductivity* 5, June 1995, pp. 1000-1003.

[3] D. Dell'Orco, et al, "Design of the $Nb_3Sn$ Dipole D20", *IEEE Trans. on Applied Superconductivity* 3, No. 1, March 1993, pp. 82-86.

[4] A.den Ouden, S. Wessel, E. Krooshoop, H.ten Kate, "Application of $Nb_3Sn$ Superconductors in High-Field Accelerator Magnets", paper LN-2 in these proceedings.